

Decoding Interfering Signals With Fewer Receiving Antennas

Zhao Li^{†*}, Xiaoqin Dai^{*}, Kang G. Shin[†]

[†]Department of Electrical Engineering and Computer Science, The University of Michigan

^{*}State Key Laboratory of Integrated Service Networks, Xidian University

zli@xidian.edu.cn, xq dai56@163.com, kgshin@eecs.umich.edu

Abstract—Due to the hierarchical structure and heterogeneity of most deployed wireless networks, multiple data transmissions using the same communication resource, such as frequency band and time slot, are likely to occur in the same area. Hence, interference becomes critical to the decoding of interfered signals. There have already been numerous techniques dealing with interferences that can be implemented either at the transmitter, the receiver or both, to support simultaneous multi-user transmissions. This paper focuses on the reception design in multiple access channels (MACs) where multiple transmitters send data to a common receiver simultaneously. By exploiting the constructive/destructive interactions among interfering signals, we propose a receiver structure based on interference combination (ICom) incorporating zero-forcing (ZF) and successive interference cancellation (SIC). The proposed receiver structure does not require coordination at the transmitter side and can significantly reduce the number of receiving antennas at a moderate processing cost. The ICom-based reception is shown to be able to not only achieve a significant improvement of system spectral efficiency (SE) under stringent latency constraints, but also make a flexible tradeoff between the requirement of receiving antennas and signal processing complexity, thus facilitating its implementation and deployment.

I. INTRODUCTION

With the rapid development of wireless communication technologies, most deployed networks are hierarchically organized. For example, small cells [1] are overlaid on top of traditional cellular systems so as to increase the frequency reuse, improve network coverage and offload traffic from macrocells. Communication networks are also heterogeneous. Multiple types of technologies, such as ad hoc, cooperative communication, device-to-device (D2D) and cognitive radio (CR), have been proposed and studied extensively. However, the hierarchical structure and heterogeneity of widely-deployed wireless networks make the interference between them more complex and difficult to manage. On one hand, when new technologies are deployed to accommodate multiple subscribers, more interference will likely be introduced. On the other hand, as the degree of frequency reuse increases, multiple co-located transmissions may share the same frequency band, thus introducing various types of co-channel interference (CCI). The interference problem must be addressed adequately, else the improvement of network performance will be limited or even impossible.

User scheduling [2] can be used to select a set of subscribers so as to simplify and handle interferences, but unscheduled subscribers will be blocked. Bursty traffic — especially in

the networks where the number and transmission demands of users vary widely and dynamically — cannot be supported. As a result, how to exploit the system capacity to accommodate as many subscribers as possible becomes a key issue. The interference caused by a user's transmission in the network is known to be a structured signal [3]. Compared to structureless noises, the interference's signature can then be exploited in the design of a transmission mechanism. Thanks to the array signal processing capability brought by multi-antenna technology, multiple interfering signals can be distinguished in the spatial domain. By generating appropriate directional beams and/or employing receive filters, interferences can be managed effectively. There have been numerous promising interference management (IM) techniques, including interference cancellation (IC) [3], interference alignment (IA) [4], interference neutralization (IN) [5], adaptive filtering, etc. With these methods, interference can be manipulated separately or jointly at the transmitter and the receiver side to recover multiple simultaneous interfering signals.

Although IA and IN emerge as promising IM methods, their applicability is still limited for the following reasons.

First, both require coordination at the transmitter side, i.e., the interferers should know the spatial feature of the desired signal so as to generate proper directional beams for IA or IN at the destination. Especially for IN, multiple interfering signals should carry the same information to neutralize them. So, simultaneously-transmitted signals should be shaped interdependently, thereby sacrificing some users' QoS for preservation of the others'. Moreover, in wireless multiple access channels, due to the capability limit and the overhead constraint of mobile terminals, non-interoperability between different operators, etc., the coordination among mobile users is expensive and not always possible.

Second, the DoF (Degree of freedom) requirement is critical to the feasibility of IA and IN. The transmitter should be equipped with multiple antennas so as to form directional beams with differentiated spatial signatures. The number of receiving antennas should also be greater than or equal to the total number of independent data streams from all transmitters, so that multiple transmissions can share time and frequency resources via spatial division multiplexing. Otherwise, system overloading will occur as the number of the transmitter's spatial DoFs exceeds that at the receiver. In such a case, the reception capability becomes the bottleneck for decoding

concurrently-transmitted data streams.

Given specific transmitter-side parameter settings, increasing the number of receiving antennas seems to be an effective way to decode more interfering signals. However, due to space limitation and hardware cost, it is impractical to increase receiving antennas beyond a certain limit, especially for mobile terminals. In the design of wireless networks, a number of concurrent transmissions to a common destination becomes popular to accommodate more subscribers and improve network capacity. For example, in uplink communications, the access point needs to decode signals from multiple subscribers. In cooperative communications, a relay node may receive its own signal and others to be forwarded simultaneously. It is, therefore, of practical importance to develop a reception mechanism that can decode multiple concurrent signals with fewer receiving antennas.

In this paper, we exploit the interactions among multiple interfering signals to reduce the number of receiving antennas while preserving the capability of recovering the interfering signals. The proposed mechanism does not require any transmitter-side cooperation, i.e., all transmitters can send signals to a common receiver without consuming any resource for the others. Thanks to the advanced signal processing capability of hardware, the reduction of receiving antennas can be compensated for via more sophisticated signal processing inside the equipments.

The main contributions of this paper are two-fold:

- Development of a reception mechanism that exploits the constructive/destructive interactions among multiple interfering signals, thus reducing the requirement of receiving antennas significantly while preserving the capability of recovering multiple concurrently-transmitted signals;
- Making a flexible tradeoff between the number of receiving antennas and the computational complexity. The complexity can be reduced further by using SIC, and an extension of the proposed reception mechanism is elaborated under more general system settings.

We will use the following notations throughout the paper. The set of complex numbers is denoted as \mathbb{C} , while vectors and matrices are represented by bold lower-case and upper-case letters, respectively. The Hermitian (or conjugate transpose), pseudo-inverse and inverse of a vector or a matrix are denoted as $(\cdot)^H$, $(\cdot)^\dagger$ and $(\cdot)^{-1}$, respectively, while $\mathbb{E}(\cdot)$ and $\|\cdot\|$ represent statistical expectation and the Euclidean norm.

II. RELATED WORKS

Interference alignment (IA) has been under development in recent years [6-10]. Its principle is to confine all interferences to a subspace of minimal dimensions at the receiver so as to maximize the available dimensions for the intended signals. Via preprocessing at the transmitter side, multiple interfering signals are mapped into a finite subspace, so that desired signal(s) may be sent through a subspace without attenuation. The authors of [6] showed that the feasibility of IA is highly dependent on system parameters, such as the numbers of transmitters and receivers, configuration of transmitting and

receiving antennas, etc. Opportunistic IA was proposed in [7] for a large number of users to harvest the multiuser diversity so as to facilitate the implementation of IA. IA-based coordinated beamforming was proposed in [8] to improve the downlink performance of multiple cell-edge users in multi-user multiple-input multiple-output (MU-MIMO) systems. IA-based uplink IM for two-tier cellular systems was devised in [9]. The author of [10] designed an IA-based uplink transmission scheme in a simple CR-MIMO systems consisting of one primary user, one secondary user and a common destination.

With IC, the previously-decoded information is subtracted from the mixed signal, and then a fewer components are left in the signal for further processing. One typical application of IC is SIC [3,11,12], which is somewhat analogous to decision feedback equalization. SIC is a multi-user detection technique that uses the structure of an interference signal to decode multiple concurrent transmissions. It can be adopted for uplink [11] and downlink [12]. Another way of applying IC is to combine it with IA, called *IAC* [13,14]. It can be applied to the scenarios where neither IA nor IC alone could be used and expected to provide more DoFs than IA.

Interference can be not only aligned but also canceled through multiple paths, which are referred to as *interference neutralization* (IN) [15-18]. IN is a new IM mechanism found from and inherent in interference networks with relays [15,16]. IN strives to properly combine signals arriving from various paths in such a way that the interfering signals are canceled while the desired signals are preserved [17]. It can be regarded as a distributed zero-forcing of interference before the interfering signal arrives at the undesired destination [18]. The authors of [17] constructed a linear distributed IN scheme that encodes in both space and time for separate multiuser uplink-downlink two-way communications. In [18], an aligned IN was proposed in a multi-hop interference network formed by concatenation of two two-user interference channels.

III. SYSTEM MODEL AND ASSUMPTIONS

As depicted in Fig. 1, the system under consideration consists of K transmitters (Tx), each with $N_T \geq 1$ antennas, and one receiver (Rx) with $N_R > 1$ antennas. Transmitters have the same transmit power P_T and are mutually independent, i.e., no transmitter-side coordination. All Txs transmit to Rx simultaneously, and the system is perfectly synchronized, i.e., signals from Txs are assumed to arrive at the destination at the same time (symbol-synchrony) [19]. This assumption was also used in some existing IN studies [15,18]. The channel matrix between an arbitrary transmitter, say Tx_k and Rx, is denoted by $\mathbf{h}_k \in \mathbb{C}^{N_R \times N_T}$, $k \in \{0, \dots, K-1\}$, whose elements are modeled as independent and identically distributed zero-mean unit-variance complex Gaussian random variables. Channel reciprocity is assumed to hold. Channels are characterized by block fading. Rx can accurately obtain all channel state information (CSI) via Txs' feedback.

For an arbitrary Tx_k , the bit stream is first mapped into transmit symbols based on a predefined constellation map. Let $\mathcal{S}_k = \{s_1, \dots, s_L\}$ denote the symbol set adopted by Tx_k .

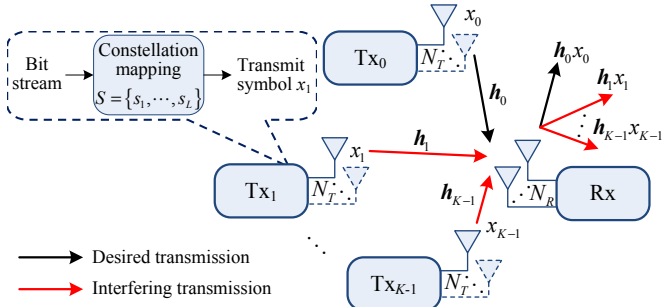


Fig. 1. System model.

For simplicity, we assume all the Txs employ an identical modulation scheme, i.e., $\mathcal{S}_k = \mathcal{S}$, $k \in \{0, \dots, K-1\}$. The size of \mathcal{S} is $|\mathcal{S}| = L$, where $|\cdot|$ represents the cardinality of a finite set. Then, the modulated symbol $x_k \in \mathcal{S}$ is mapped onto and sent by N_T antennas of Tx_k . If $N_T > 1$, precoding may be applied, i.e., x_k is multiplied by a selected weight vector before it is sent out. So, the direction of a transmitted signal can be controlled to enhance communication performance.

Since our focus is on the design of a reception mechanism, for simplicity we assume each source node is equipped with a single antenna in the following discussion. This is in some sense a worst-case assumption, since there is no coordination among the transmitting antennas. However, the proposed scheme can be easily extended to the case of $N_T > 1$. Under such condition, one or more directional beams corresponding to beamforming (BF) and spatial multiplexing (SM), respectively, can be sent by a transmitter. The transmit power of each Tx, P_T is equally allocated to the beams. If BF is employed at Tx_k , we have $\mathbb{E}(\|x_k\|^2) = P_T$, else $\mathbb{E}(\|\mathbf{x}_k\|^2) = P_T$ where \mathbf{x}_k denotes the transmitted symbol vector. However, in this paper we assume only one data stream is sent by a Tx irrespective of N_T which is in accordance with our main concern.

According to the system model, the common receiver needs to decode all the signal components sent from K Txs. As shown in Fig. 1, we take x_0 's recovery as an example, and treat the other $K-1$ signals carrying x_1, \dots, x_{K-1} as interferences.

IV. DESIGN OF A MAC RECEIVER WITH FEWER RECEIVING ANTENNAS

By exploiting the constructive/destructive interactions among interfering signals, we can reduce the required number of receiving antennas significantly. We first propose ICom-based signal processing for decoding multiple interfering signals, and then present a MAC receiver structure based on ICom. For the clarity of exposition, these are discussed based on some simplified parameter settings which is followed by a generalized design. Finally, the associated computational complexity is analyzed.

A. ICom-based signal processing

We first describe some basic signal processing algorithms that could be employed in MAC receiver design, including matched filter (MF) and zero-forcing (ZF), and then propose

the ICom-based ZF. The following discussion is for the case of $N_T = 1$; if $N_T > 1$ and precoding is employed, the actual spatial signature of a signal should be used. Let's consider x_0 's decoding in Fig. 1 as an example. Then, the received signal at Rx can be expressed as:

$$\mathbf{y} = \mathbf{h}_0 x_0 + \sum_{k=1}^{K-1} \mathbf{h}_k x_k + \mathbf{n} \quad (1)$$

where the first term on the right-hand side (RHS) of Eq. (1) is the intended signal, the second term represents for the sum of interferences from the other $(K-1)$ Txs. \mathbf{n} is an additive white Gaussian noise (AWGN) vector, elements of which have mean 0 and variance σ_n^2 . In order to decode x_0 , Rx applies the filter vector \mathbf{w}_0 to obtain the estimated signal:

$$\hat{y} = \mathbf{w}_0^H \mathbf{h}_0 x_0 + \mathbf{w}_0^H \sum_{k=1}^{K-1} \mathbf{h}_k x_k + \mathbf{w}_0^H \mathbf{n}. \quad (2)$$

\mathbf{w}_0 can be designed as $\mathbf{w}_0 = \mathbf{f}_0^M = \mathbf{h}_0 / \|\mathbf{h}_0\|$ — called the *matched filter* (MF). So, the receiving power of the desired signal can be maximized, but the interference term remains. The other way to design \mathbf{w}_0 is to project \mathbf{h}_0 — the spatial feature of the desired signal — onto the orthogonal space spanned by the orthonormal bases derived from \mathbf{h}_k , i.e., the spatial signature of signals from the other Txs. Then, the interference could be nullified at Rx. This type of filter, known as *zero-forcing* (ZF), is characterized by the orthogonal subspace projection, hence represented as \mathbf{f}_0^O . With \mathbf{f}_0^O , effective power loss relative the desired signal results since $\|(\mathbf{f}_0^O)^H \mathbf{h}_0\| = \|\mathbf{h}_0\|$ cannot be guaranteed. In order to obtain \mathbf{f}_0^O , we first apply Gram-Schmidt [20] to $\mathbf{h}_1, \dots, \mathbf{h}_{K-1}$ to obtain a set of orthonormal bases $\tilde{\mathbf{h}}_1, \dots, \tilde{\mathbf{h}}_{K-1}$. Then, \mathbf{f}_0^O is computed as:

$$\mathbf{f}_0^O = \frac{\mathbf{h}_0 - \sum_{k=1}^{K-1} \tilde{\mathbf{h}}_k^H \mathbf{h}_0 \tilde{\mathbf{h}}_k}{\left\| \mathbf{h}_0 - \sum_{k=1}^{K-1} \tilde{\mathbf{h}}_k^H \mathbf{h}_0 \tilde{\mathbf{h}}_k \right\|}. \quad (3)$$

Note that $N_R \geq K$ should be satisfied so as to calculate \mathbf{f}_0^O . However, in practice, the number of Txs is always greater than N_R . Without users' scheduling, the solution of \mathbf{f}_0^O will not be available due to insufficient DoFs of the Rx.

By exploiting the fact that multiple interfering signals from K single-antenna Txs interact, i.e., construct or destruct with each other upon their arrival at Rx, we can design a filter as follows. First, the $K-1$ interferences are combined to produce an effective interference, whose spatial signature is defined by $\tilde{\mathbf{h}}_\epsilon = \sum_k \mathbf{h}_k x_k / \|\sum_k \mathbf{h}_k x_k\|$, i.e., $\tilde{\mathbf{h}}_\epsilon$ is determined by both the channel status and the transmitted symbols w.r.t. the $K-1$ interferers. Then, the ICom-based filter, denoted by \mathbf{g}_0^O , can be readily obtained by projecting \mathbf{h}_0 onto the perpendicular direction w.r.t. $\tilde{\mathbf{h}}_\epsilon$, and then applying normalization to the result as:

$$\mathbf{g}_0^O = \frac{\mathbf{h}_0 - \tilde{\mathbf{h}}_\epsilon^H \mathbf{h}_0 \tilde{\mathbf{h}}_\epsilon}{\left\| \mathbf{h}_0 - \tilde{\mathbf{h}}_\epsilon^H \mathbf{h}_0 \tilde{\mathbf{h}}_\epsilon \right\|} \quad (4)$$

N_R should be greater than or equal to K for the existence of the solution of \mathbf{f}_0^O . For the clarity of presentation, we first take $\mathcal{S} = \{s_1, s_2\}$ (i.e., BPSK (Binary phase-shift keying)) as an example. If $x_1 = x_2 \in \mathcal{S}$ during

the current symbol transmission period, we have $\tilde{\mathbf{h}}_\varepsilon = (\mathbf{h}_1 x_1 + \mathbf{h}_2 x_2) / \|\mathbf{h}_1 x_1 + \mathbf{h}_2 x_2\| = (\mathbf{h}_1 + \mathbf{h}_2) / \|\mathbf{h}_1 + \mathbf{h}_2\|$. Otherwise, $x_1 = -x_2$. Then, $\tilde{\mathbf{h}}_\varepsilon = (\mathbf{h}_1 - \mathbf{h}_2) / \|\mathbf{h}_1 - \mathbf{h}_2\|$ is obtained. That is, an effective interference can be obtained by combining the interfering signals. Then, the filter only needs to be orthogonal to the signature of such an interference. In other words, the interference dimension can be significantly reduced, especially when there are many interferers.

Based on the above discussion, one desired signal (e.g., x_0 among K) can be decoded with either traditional ZF (\mathbf{f}_0^O) or ICom-ZF-based reception (\mathbf{g}_0^O). With the classical ZF, $N_R \geq K$ should be satisfied to calculate \mathbf{f}_0^O . With ICom-ZF, since the dimension of interference is reduced to 1 irrespective of the number of interferers, two Rx-antennas are enough to decode x_0 . Both ZF and ICom-ZF are characterized by interference nulling and can be used in decoding multiple interfering signals. In order to recover K signals, each signal component is regarded, in turn, as the desired, and the remainders as interferences. By repeating the above process, a set of \mathbf{f}_k^O and \mathbf{g}_k^O can be obtained.

Note that in the above analysis, we assume $N_T = 1$. When $N_T > 1$ and precoding is employed, \mathbf{h}_k should be replaced by the signal's actual spatial feature, i.e., precoding information incorporated with \mathbf{h}_k is used.

B. ICom-based receiver structure

In this subsection, we first design the ICom-ZF based receiver structure and then use SIC to reduce computational complexity. We omit the superscript O in the following discussion for clarity of exposition, and assume $N_T = 1$ without loss of generality.

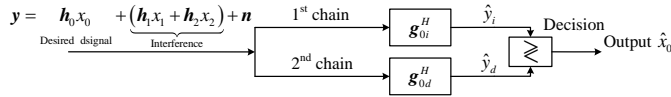


Fig. 2. Structure of an ICom-ZF receiving branch with $K = 3$, $N_R = 2$ and $L = 2$.

We begin with $L = 2$ and assume that the elements of \mathcal{S} are symmetric about the origin. Since the sum of $\mathbf{h}_k x_k$ determines the spatial feature of an effective interference, with $L = 2$, there will be 4 symbol combination types, i.e., effective interferences. However, due to the symmetric feature of the elements of \mathcal{S} , only 2 cases — i.e., identical and different phases — need to be considered. Taking x_0 's decoding as an example, with $K = 3$ and $N_R = 2$, Fig. 2 shows the structure of an ICom-ZF receiving branch. The subscript i and d indicate *identical* and *different* transmitted symbols, respectively.

In Fig. 2, \mathbf{g}_{0i} and \mathbf{g}_{0d} is calculated by substituting $\tilde{\mathbf{h}}_\varepsilon = (\mathbf{h}_1 + \mathbf{h}_2) / \|\mathbf{h}_1 + \mathbf{h}_2\|$ and $\tilde{\mathbf{h}}_\varepsilon = (\mathbf{h}_1 - \mathbf{h}_2) / \|\mathbf{h}_1 - \mathbf{h}_2\|$ into Eq. (4), respectively. If the actual symbol combination is in accordance with the first chain where $x_1 = x_2$ is assumed, we have $\mathbf{g}_{0i}^H (\mathbf{h}_1 + \mathbf{h}_2) = 0$ and the interference is thus mitigated. The estimated $\hat{y}_i = \mathbf{g}_{0i}^H \mathbf{h}_0 x_0 + \mathbf{g}_{0i}^H \mathbf{n}$. Then, the achievable signal-to-noise ratio (SNR) is computed as:

$$\gamma_{0i} = \frac{P_T (\mathbf{g}_{0i}^H \mathbf{h}_0) (\mathbf{g}_{0i}^H \mathbf{h}_0)^H}{\sigma_n^2} \quad (5)$$

However, in the second chain $\mathbf{g}_{0d}^H (\mathbf{h}_1 - \mathbf{h}_2) \neq 0$. The estimation of \hat{y}_d is:

$$\begin{aligned} \hat{y}_d &= \mathbf{g}_{0d}^H \mathbf{h}_0 x_0 + \mathbf{g}_{0d}^H (\mathbf{h}_1 x_1 + \mathbf{h}_2 x_2) + \mathbf{g}_{0d}^H \mathbf{n} \\ &= \mathbf{g}_{0d}^H \mathbf{h}_0 x_0 + 2\mathbf{g}_{0d}^H \mathbf{h}_2 x_1 + \mathbf{g}_{0d}^H \mathbf{n} \end{aligned} \quad (6)$$

x_1 can also be replaced by x_2 since they are identical. The output signal-to-interference-plus-noise ratio (SINR) of the second chain is then:

$$\gamma_{0d} = \frac{P_T (\mathbf{g}_{0d}^H \mathbf{h}_0) (\mathbf{g}_{0d}^H \mathbf{h}_0)^H}{\sigma_n^2 + 4P_T (\mathbf{g}_{0d}^H \mathbf{h}_2) (\mathbf{g}_{0d}^H \mathbf{h}_2)^H} \quad (7)$$

One can see that the interference part still remains in Eq. (7). Both \hat{y}_i and \hat{y}_d are sent to the decision module, then by making a SNR/SINR comparison, \hat{x}_0 can be obtained via demodulating the chain without interference.

If $x_1 = -x_2$, $\mathbf{g}_{0d}^H (\mathbf{h}_1 - \mathbf{h}_2) = 0$, whereas $\mathbf{g}_{0i}^H (\mathbf{h}_1 - \mathbf{h}_2) \neq 0$. The output $\hat{y}_d = \mathbf{g}_{0d}^H \mathbf{h}_0 x_0 + \mathbf{g}_{0d}^H \mathbf{n}$. Similarly to the derivation of Eq. (6), \hat{y}_i is given as:

$$\hat{y}_i = \mathbf{g}_{0i}^H \mathbf{h}_0 x_0 - 2\mathbf{g}_{0i}^H \mathbf{h}_2 x_1 + \mathbf{g}_{0i}^H \mathbf{n} \quad (8)$$

As for the decoding of x_1 and x_2 , the same structure illustrated in Fig. 2 can be directly applied. What we need to do are replacing the desired data x_0 by x_1 and x_2 , respectively, redesigning the filter as described in the last subsection, and implementing the ICom-ZF branch repeatedly. Although the above design is with $K = 3$, by duplicating the reusable processing module, it can be easily extended to a general K .

Given $L = 2$, general N_R and $K > N_R$, since the number of decodable signals using the above ICom-ZF receiving branch is $N_R - 1$, the number of required chains becomes $2^{K-(N_R-1)-1} = 2^{K-N_R}$. Here, we exploit the symmetric property of the elements of \mathcal{S} so that the number of symbol combinations can be reduced by a factor of 1/2. With ICom-ZF, the filter vector in the ι^{th} chain of a branch for decoding x_k , denoted by $\mathbf{g}_{k\iota}$, can be obtained by projecting \mathbf{h}_k onto the orthogonal subspace spanned by an orthonormal bases derived from $[\mathbf{h}_0 \cdots \mathbf{h}_{k-1} \mathbf{h}_{k+1} \cdots \mathbf{h}_{N_R-2} \sum_{k'=N_R-1, k' \neq k}^{K-1} \mathbf{h}_{k'} x_{k'}]$, or equivalently computing the inverse of $\mathbf{H} = [\mathbf{h}_0 \cdots \mathbf{h}_{N_R-2} \sum_{k'=N_R-1, k' \neq k}^{K-1} \mathbf{h}_{k'} x_{k'}]$ and take the transpose of the k^{th} row vector, and then applying normalization to the result. The subscript ι could be either i or d_π ($\pi = 1, \dots, 2^{K-N_R} - 1$), indicating one identical- ($\iota = i$) or $2^{K-N_R} - 1$ different-symbol combinations, respectively.

To make further generalization, when $L > 2$, a new dimension related to modulation is introduced in addition to K and N_R which will cooperatively affect the computational complexity (the number of chains in a branch). In general, the increase of L and K will incur more processing load, whereas increasing N_R will reduce computational complexity at the expense of larger receiver size and more hardware cost. For K single-antenna sources transmitting to a common destination equipped with $N_R \geq 2$ antennas, and each source employing the constellation map whose size is as large as L , there will be at most $K - (N_R - 1)$ un-decodable signal components in the above ICom-based decoding branch. Suppose the elements

TABLE I
REQUIREMENT OF VIRTUAL CHAINS FOR DIFFERENT K , N_R AND $L = 2$.

K	N_R	w/o SIC		w/ SIC	
		No. of required VCs	No. of decodable signals	No. of required VCs	No. of decodable signals
2	2	$1 \times VC_\beta$	2	$1 \times VC_\beta$	2
3	2	$2 \times VC_\alpha$	1	$2 \times VC_\alpha$	1
		$4 \times VC_\alpha$	2	$2 \times VC_\alpha + 1 \times VC_\beta$	3
		$6 \times VC_\alpha$	3	—	—
4	2	$4 \times VC_\alpha$	1	$4 \times VC_\alpha$	1
		$8 \times VC_\alpha$	2	$6 \times VC_\alpha$	2
		$12 \times VC_\alpha$	3	$6 \times VC_\alpha + 1 \times VC_\beta$	4
		$16 \times VC_\alpha$	4	—	—
3	3	$1 \times VC_\beta$	3	$1 \times VC_\beta$	3
4	3	$2 \times VC_\alpha$	2	$2 \times VC_\alpha$	2
		$4 \times VC_\alpha$	4	$2 \times VC_\alpha + 1 \times VC_\beta$	4
K	N_R	$\mu 2^{K-N_R} \times VC_\alpha$	$\min\{\mu(N_R-1), K\}$	$\sum_{m=1}^{\eta} \{\varphi_\alpha 2^{K-m(N_R-1)-1} \times VC_\alpha\} + \varphi_\beta \times VC_\beta$	$\min\{\eta(N_R-1) + \varphi_\beta N_R, K\}$

in \mathcal{S} are symmetric about the origin, e.g., QAM (Quadrature amplitude modulation), then the number of chains required in a branch is $\frac{1}{2}L^{K-(N_R-1)}$.

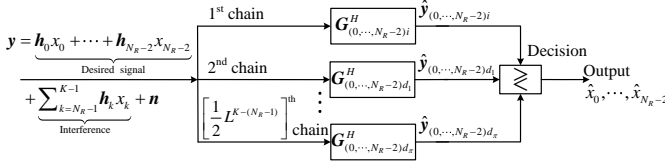


Fig. 3. Structure of an ICom-ZF receiving branch for general K , N_R and L .

Fig. 3 illustrates the structure of ICom-ZF receiving branch for general K , N_R and L . $\pi = \frac{1}{2}L^{K-(N_R-1)} - 1$ is used to denote the number of chains corresponding to different symbol combinations. Matrix $\mathbf{G}_{\mathcal{A}l}$ consists of $N_R - 1$ ZF-based filter vectors \mathbf{g}_{kl} , where \mathcal{A} represents an array and $k \in \mathcal{A}$.

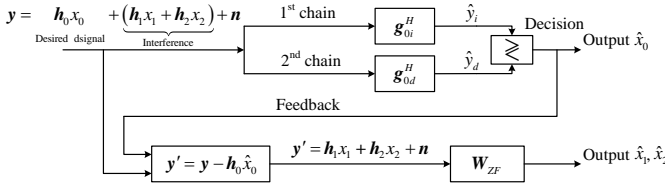


Fig. 4. Structure of ICom/SIC-ZF receiver for $K = 3$, $N_R = 2$ and $L = 2$.

With large K and L but a small N_R , repeating the above module would impose a huge computation load on the receiver. We employ SIC to reduce this computational load. With SIC, the interference from already-detected components of a transmitted symbol vector is subtracted from the received signal vector, yielding a modified received vector in which fewer interferers are present [3]. So, we need not repeat the module given in Fig. 2 or 3 multiple times in order to decode all the signal components. Instead, we adopt the structure shown in Fig. 4. For simplicity, we use the parameter settings $K = 3$, $N_R = 2$ and $L = 2$ to illustrate the application of SIC. This can be easily extended to more generalized cases. From the figure, by employing the decision feedback information \hat{x}_0 , the signal component carrying x_0 can be subtracted from the received signal \mathbf{y} . We assume $\hat{x}_0 = x_0$, i.e., decoding is error-free. Note that after interference cancellation, the number of signals is reduced to 2, which is not greater than N_R any

longer. Then, a traditional ZF receiver $\mathbf{W}_{ZF} = (\overline{\mathbf{H}}^H \overline{\mathbf{H}})^{-1} \overline{\mathbf{H}}^H$ where $\overline{\mathbf{H}} = [\mathbf{h}_1 \ \mathbf{h}_2]$ can be directly applied to the residual mixed signal \mathbf{y}' to recover \hat{x}_1 and \hat{x}_2 .

Table I illustrates the tradeoff between the required N_R and the processing complexity for the case of $L = 2$. For simplicity, we use a *virtual chain* (VC) to represent the computational complexity. An α -type VC, denoted by VC_α , is defined as the structure shown in Fig. 3, whereas one β -type VC (VC_β) is equivalent to a traditional ZF. In Table I, the variable $\mu = 1, 2, \dots, \lceil \frac{K}{N_R-1} \rceil$ where $\lceil \cdot \rceil$ denotes rounding the element to the nearest integer greater than or equal to it. $\eta = 1, 2, \dots, \lceil \frac{K-N_R}{N_R-1} \rceil + 1$ represents for the number of ICom-ZF branch incorporating with SIC. $\varphi_\alpha = \begin{cases} 1, & \text{if } m \leq \lceil \frac{K-N_R}{N_R-1} \rceil \\ 0, & \text{Otherwise} \end{cases}$, $\varphi_\beta = \begin{cases} 0, & \text{if } \eta \leq \lceil \frac{K-N_R}{N_R-1} \rceil \\ 1, & \text{Otherwise} \end{cases}$. The table shows that with SIC, the receiver structure is reduced significantly, compared to the one without SIC. We can make a flexible tradeoff between N_R and processing complexity.

When $N_T > 1$, multiple data streams may be sent by one Tx, and the title of the first column in Table I should be the number of transmitted signals. When $K = N_R$, for both schemes, without or with SIC, the classical ZF reception can be directly applied. When $K > N_R$, the DoFs at Rx are insufficient for decoding all the signal components at once, and hence the proposed ICom-based reception scheme can be employed. With a general L , the base number 2 in Table I should be replaced by L . Moreover, in practical use Txs may employ different modulation schemes adaptively. Then some feedback mechanisms are required so that Rx is able to acquire the transmission parameters of the Txs, based on which the receiver structure is dynamically configured following the concept of software defined radio (SDR). For space limitation, the detailed discussion is omitted.

C. Analysis of computational complexity

The complexity is quantified in number of real floating point operations (flops) [20]. A real addition, multiplication, or division is counted as one flop. A complex addition and multiplication have two flops and six flops, respectively.

We need $\lceil \frac{K-N_R}{N_R-1} \rceil + 1$ stages in total to decode K signals with N_R antennas. In each chain of the first $\lceil \frac{K-N_R}{N_R-1} \rceil$ stages, the computation includes the calculation of filter matrix $\mathbf{G}_{\mathcal{A}l}^H$

and multiplication of $\mathbf{G}_{\mathcal{A}_L}^H$ with the received mixed signal. In order to obtain $\mathbf{G}_{\mathcal{A}_L}^H$, we first use Gauss-Jordan elimination to compute the inverse of an $N_R \times N_R$ matrix $\bar{\mathbf{H}}$. This operation takes N_R^3 complex multiplications/divisions and $N_R(N_R - 1)^2$ complex additions. Then, the first $N_R - 1$ row vectors of $\bar{\mathbf{H}}^{-1}$ are normalized to compose $\mathbf{G}_{\mathcal{A}_L}^H$. Frobenius norm of a $1 \times N_R$ vector takes $4N_R$ flops, and the normalization takes N_R complex divisions, so the flop count for normalizing a $(N_R - 1) \times N_R$ matrix is $10N_R(N_R - 1)$. Next, the mixed $N_R \times 1$ signal is left multiplied by $\mathbf{G}_{\mathcal{A}_L}^H$ which takes $N_R(N_R - 1)$ complex multiplications and $(N_R - 1)^2$ complex additions. Based on the above analysis, the complexity of an arbitrary chain in the first $\lceil \frac{K-N_R}{N_R-1} \rceil$ stages is $8N_R^3 + 14N_R^2 - 18N_R + 2$. In each stage $m \leq \lceil \frac{K-N_R}{N_R-1} \rceil$, the outputs of $\xi = \frac{1}{2}L^{K-(N_R-1)}$ $L^{-(m-1)(N_R-1)}$ chains, each of which contains $N_R - 1$ real SNRs or SINRs, are compared with each other to find the maximum value. This operation takes $(N_R - 2)\xi$ real additions and $\xi - 1$ real subtractions. As a result, the complexity of the m^{th} stage is $(8N_R^3 + 14N_R^2 - 17N_R + 1)\xi - 1$.

In the last stage, the number of signal components, say ψ , is no greater than N_R , and thus traditional ZF can be directly applied and no SNR/SINR comparison is needed. When $\psi = N_R$, the operations in the final stage include the inversion of an $N_R \times N_R$ signal feature matrix, normalization of the inverse matrix, and multiplication of the $N_R \times N_R$ filter matrix with an $N_R \times 1$ mixed signal, which take $8N_R^3 - 4N_R^2 + 2N_R$, $10N_R^2$ and $8N_R^2 - 2N_R$ flops, respectively. The total flop count is $8N_R^3 + 14N_R^2$. When $\psi < N_R$, the pseudo-inverse of an $N_R \times \psi$ matrix, denoted by $\bar{\mathbf{H}}$ is required. According to the pseudo-inverse calculation $\bar{\mathbf{H}}^\dagger = (\bar{\mathbf{H}}^H \bar{\mathbf{H}})^{-1} \bar{\mathbf{H}}^H$, two matrix multiplications and one matrix inversion are needed, which takes $16\psi^2 N_R + 8\psi^3 - 6\psi^2 - 2\psi N_R + 2\psi$ flops. Additionally, by taking into account the normalization of filter matrix and multiplication of \mathbf{W}_{ZF} with mixed signal, of which the flop counts are $10\psi N_R$ and $8\psi N_R - 2\psi$ respectively, the computational complexity of the last stage under $\psi < N_R$ is $16\psi^2 N_R + 8\psi^3 - 6\psi^2 + 16\psi N_R$.

Based on the above discussion, the total computational complexity of the proposed scheme in flops can be approximately computed by $N_R^3 L^{K-(N_R-1)} \sum_{m=1}^{\lceil \frac{K-N_R}{N_R-1} \rceil} L^{-(m-1)(N_R-1)}$.

V. EVALUATION

We use simulation with MATLAB to demonstrate the performance of the proposed reception mechanism. K TxS and one common Rx are used for the simulation. Each Tx is equipped with N_T antennas and sends a single data stream with power P_T . Rx has N_R antennas. When $N_T = 1$, Tx sends omnidirectionally. Otherwise, Tx employs singular value decomposition (SVD) based precoding in terms of its channel status with the destination, and adopts the principle eigen-mode to transmit to Rx. Precoders and receive filters should be normalized for power gain fairness. The following two subsections will cover the evaluation of system spectral efficiency (SE) and delay performance.

A. Spectral efficiency

We simulate the proposed ICom/SIC-ZF as well as four other methods including MF, traditional ZF, IA, and IN for comparison of their SE. With the MF, a total of K filter vectors each of which matches a desired signal are generated by Rx and combined to form a filter bank, and K signals are then decoded. The SINR of the k^{th} ($k \in \{0, \dots, K-1\}$) desired signal can be obtained as $\gamma_k^M = \frac{P_T \|(\mathbf{f}_k^M)^H \mathbf{h}_k\|^2}{P_T \sum_{k'=0, k' \neq k}^{K-1} \|(\mathbf{f}_k^M)^H \mathbf{h}_{k'}\|^2 + \sigma_n^2}$, where \mathbf{f}_k^M denotes the MF for the signal from Tx _{k} and \mathbf{h}_k represents the signal feature that may include precoding information when Tx _{k} is equipped with multiple antennas. When $K \leq N_R$, all of the K signals can be recovered by employing ZF, thus making IA, IN and ICom/SIC-ZF unnecessary. That is, ICom/SIC-ZF has advantages over the classical ZF only when $K > N_R$. Under such condition, IA, IN and ICom/SIC-ZF are implemented, respectively, as follows.

- With IA, $K - (N_R - 1)$ of K signals are randomly selected and adjusted to align in one direction so that the rest of $N_R - 1$ signals may be decoded by applying ZF. The performance of IAC can be referred to that of IA since it decodes the same number of signals as IA.
- IN can be employed to recover N_R signals. In the simulation, we randomly pair signals originating from the $K - N_R$ transmitters. Then, in each pair, we adjust the signal with a higher channel gain to neutralize the one with lower gain so that additional power cost can be avoided. Note that when $K - N_R$ is an odd number, one Tx will be left unpaired—we simply turn off this Tx to eliminate its interference.
- As for ICom/SIC-ZF, $K - (N_R - 1)$ signals are first randomly selected and treated as an effective interference. ZF is then employed to decode the other $N_R - 1$ signals. By combining with SIC, all K signals can be recovered successively.

For conciseness, we will use a general form $[N_T \ N_R \ K \ K_d]$ to denote the parameters for different methods, where K_d is the number of decodable signals for given N_T , N_R and K . Figs. 5–7 show the impacts of K , N_T and N_R on the system SE, respectively. In order to show the advantage of proposed ICom/SIC-ZF, the simulation in Figs. 5–7 is under $K > N_R$. However, in such a case traditional ZF is not applicable. Fig. 8 plots the system SE for different K s satisfying the minimum antenna requirement for recovering all K signals.

Fig. 5 shows the system SE of different schemes with fixed N_T , N_R and different K s. Note that both IA and IN require at least 2 Tx-antennas, so we set $N_T = 2$, $N_R = 3$ and $K \in \{4, 5, 6\}$. Note that with IA, IN and ICom-ZF, the decoded signals are interference-free, whereas with MF, CCI exists. When $K > N_R$, K_d with IA and IN is limited by N_R , and hence their SE is independent of K . Specifically, IN can recover N_R signals while IA only decodes $N_R - 1$. As a result, IN yields a higher SE than IA. On the other hand, both MF and ICom/SIC-ZF can decode K signals without any constraint on N_R , but ICom/SIC-ZF can eliminate CCI, whereas MF

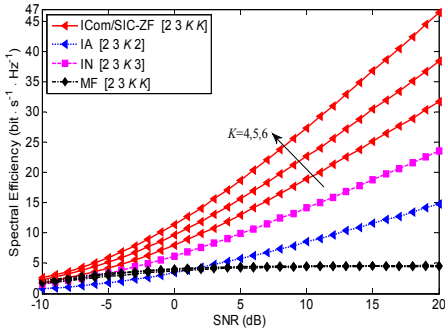


Fig. 5. System SE with fixed N_T , N_R and different K .

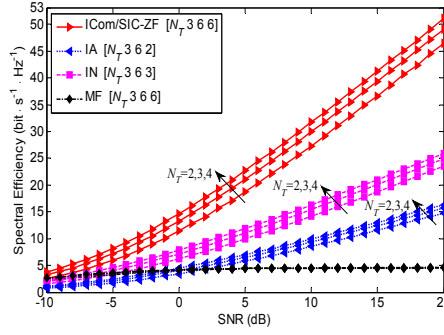


Fig. 6. System SE with fixed N_R , K and different N_T .

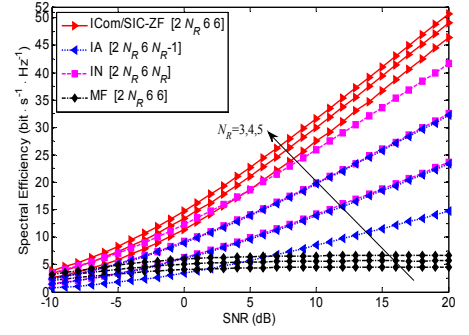


Fig. 7. System SE with fixed N_T , K and different N_R .

cannot. As K increases, K_d of MF and ICom/SIC-ZF grows, improving system SE. But with MF, the aggregate interference $\sum_{k'=0, k' \neq k}^{K-1} \|(\mathbf{f}_k^M)^H \mathbf{h}_{k'}\|^2$ for user k becomes stronger and hence degrades the system SE. From the expression of γ_k^M , we can see that when SNR is low, noise dominates the achievable SE, and MF maximizes the effective power of intended signal, thus improving its SE as SNR gets higher. Given an extremely low SNR, IA and IN cannot achieve an obvious gain from interference management. In contrast, MF can gain from supporting multiple Tx. Thus, under a very low SNR, MF slightly outperforms IA and IN. When SNR becomes higher, the interference becomes the dominant factor in limiting SE. MF cannot eliminate CCI, so γ_k^M saturates at a high SNR with fixed K and is inversely proportional to K for a given SNR. As can be seen from Fig. 5, in a high SNR region, MF's SE saturates and does not vary with K . ICom/SIC-ZF can mitigate interference, making its SE superior to the other three methods and increase with K .

Fig. 6 shows the SE of IA, IN, MF and ICom/SIC-ZF with fixed K , N_R and different N_T . We set $N_R = 3$, $K = 6$ and $N_T \in \{2, 3, 4\}$. One can see that the SE of IA, IN and ICom/SIC-ZF improves as N_T grows, because the above methods achieve interference-free reception, and a large N_T yields a higher transmit diversity gain. Since ICom/SIC-ZF decodes more signals than IN or IA, it yields much higher SE. As for MF, CCI cannot be eliminated. Increasing N_T affects both the desired signal and the interference which counteract with each other so that MF's SE is independent of N_T .

Fig. 7 shows the SE of different methods for fixed K , N_T , and different N_R . We set $N_T = 2$ to be able to utilize IA and IN, and also meet the inequality $K > N_R$. Based on the above consideration, we choose $K = 6$ and $N_R \in \{3, 4, 5\}$. Since a larger N_R introduces a higher receive diversity gain, the achievable system SE grows as N_R increases. IA and IN can recover $N_R - 1$ and N_R interference-free signals under the condition of $K > N_R$. Since IN can support one more data transmission than IA, its SE is better than IA's. When SNR is low, noise is the dominant factor affecting the system SE. Although ICom/SIC-ZF, IA and IN can eliminate interference by adopting ZF at Rx, the desired signal power suffers loss which may outweigh the benefit of interference mitigation. As a result, the achievable SE of MF approximates or even outperforms that of the other three methods in a low SNR

region. As SNR grows larger, the SE of MF saturates and becomes inferior to that of the other methods.

Fig. 8 plots system SE for different K 's satisfying the minimum antenna requirement for recovering all K signals. We only study MF, ZF and ICom/SIC-ZF because under $K > N_R$, neither IA nor IN can decode all the K signals while for $K \leq N_R$, ZF is adopted, instead of IA, IN and ICom/SIC-ZF. Since MF, ZF and ICom/SIC-ZF do not have any requirement for multiple Tx-antennas, we simply set $N_T = 1$. K is selected from the set $\{3, 4, 5\}$. From Fig. 8 we can see that with ZF and ICom/SIC-ZF, the system SE grows with K . Provided with the same K , ZF outputs the best SE since its Rx has K antennas whereas the other two methods only use 2 antennas. ICom/SIC-ZF can decode K interference-free signals, so its SE performance ranks the second. MF improves its achievable SE with SNR in a low SNR region, which saturates at high SNR, and is independent of K . The analysis is the same as that in Fig. 5.

It should be noted that in the above evaluation, error-propagation is not considered, hence SE of the proposed scheme increases with K . When the decoding is imperfect, the latter decoded signal undergoes more suboptimal filters so that its SE is deteriorated, rendering the saturation of system's SE at higher K . This can be studied in our future work.

B. Latency

We now study the tradeoff between N_R and K , as well as the modulation order L under a certain delay constraint. The latency includes processing delay (D_p) which is determined by the reception algorithm's complexity and the processor's capability at the receiver, and transmission delay (D_t) which depends on the volume of traffic, bandwidth, and received SNR/SINR. For traditional ZF, IA and IN, they have a *hard* capacity which is subject to the system's DoFs, whereas for MF and the proposed ICom/SIC-ZF, the capacity has a *soft* feature, i.e., the number of accommodated users is independent of N_R .

As for D_p , we take 100ms as the latency bound for users traffic [21]. Based on the achievable processing speed of the base station, 76.8Gflops [22], and a mobile station, from several to tens of Gflops [23], we use 1Gflops as a reference processing speed in the following evaluation. Fig. 9 shows a total D_p of $K = 10$ signals under different N_R and L .

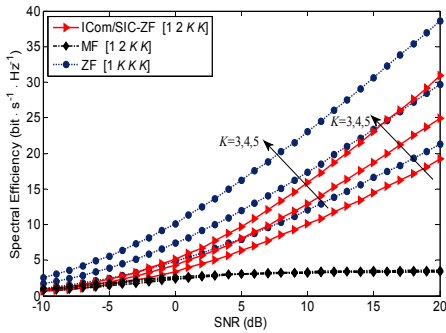


Fig. 8. System SE under minimum antenna requirement and different K s.

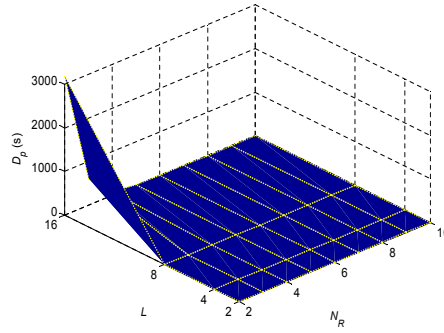


Fig. 9. Total processing delay with $K = 10$, different N_R and L .

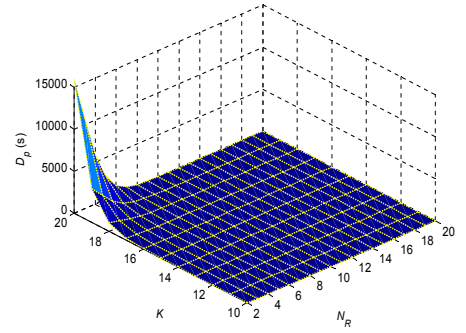


Fig. 10. Total processing delay with $L = 4$, different K and N_R .

BPSK, QPSK, and 16-QAM are considered. Note that for signals decoded in the front stages, their D_p values are smaller than the results given in Fig. 9. As shown in the figure, D_p increases with L and decreases with N_R . Assuming $L > 8$ and $N_R \leq 4$, D_p is too large to be acceptable. In this case, either increasing N_R or reducing the number of simultaneously supported users is the feasible way to guarantee that each user's D_p is under the given threshold. Fig. 10 plots the total D_p under different K and N_R . All users are assumed to adopt QPSK. D_p increases with K and decreases with N_R . Under $K > 16$ and $N_R \leq 8$, D_p becomes unacceptable. In order to decrease D_p , we can either increase N_R or reduce K .

Fig. 11 shows the requirement of N_R under the 100ms D_p -constraint, different L and K . BPSK, QPSK, 8PSK, 16-QAM and 64-QAM are considered. Given $L \leq 16$ and $K \leq 18$, at least 2 Rx-antennas can be saved with the proposed reception mechanism. When $K = 10$ and $L = 4$, only 2 Rx-antennas are required to support all the users simultaneously. However, when a high order modulation (e.g., $L \geq 64$) is employed, the traditional ZF should be directly adopted since no Rx-antenna savings can be achieved.

Since WLANs have been widely deployed, we adopt IEEE 802.11ac, an emerging WLANs protocol, as an example to evaluate the delay (D_t) performance of different schemes. By assuming that each user uses 20MHz bandwidth to send a single spatial stream to the access point, the achievable data rates under different modulation and coding schemes (MCS) are given in Table II [24]. With traditional ZF, IA and IN, K users are assumed to fairly share the system's DoFs via user scheduling such as round-robin [25], etc., so that the effective bandwidth of each user is the total system bandwidth divided by K . In contrast, with MF and ICom/SIC-ZF, each user exclusively uses the system bandwidth. Provided that all users have the same transmit power and experience statistically identical channel fading, traditional ZF, IA, IN and ICom/SIC-ZF yield the same user's spectral efficiency, since they all mitigate CCI, and hence outperform MF. We denote the system bandwidth, an arbitrary user's data volume and its SE as W , V , and C , respectively. By omitting other types of latency introduced by channel estimation, user scheduling, etc., D_t of a user with ZF, IA and IN is given as $KV/(N_R WC)$. With ICom/SIC-ZF, one user's D_t is computed as $V/(WC)$. In practice, K is always greater than N_R , so D_t of ICom/SIC-

ZF is smaller than that of traditional ZF, IA and IN. Without loss of generality, we only evaluate D_t of traditional ZF and ICom/SIC-ZF in the following.

TABLE II
IEEE 802.11ac MCS VALUES AND DATA RATES.

MCS index	Modulation	Code rate	20MHz data rate
0	BPSK	1/2	7.2Mbps
1	QPSK	1/2	14.4Mbps
3	16-QAM	1/2	28.9Mbps
5	64-QAM	2/3	57.8Mbps

Fig. 12 plots D_t of traditional ZF and the proposed ICom/SIC-ZF under the 100ms D_p -constraint. The traffic volume (V) of each user's session is assumed to be 100Mb. For a fair comparison, both strategies are simulated with the same N_R . According to Table II, data rate (WC) grows as L increases, so delays (D_t) of both schemes decrease accordingly. With the D_p -constraint, the minimum N_R of ICom/SIC-ZF with different K s can be found from Fig. 11. It can be seen from Fig. 12 that the curve of D_t of ICom/SIC-ZF is below that of ZF. Moreover, with ICom/SIC-ZF, when BPSK is adopted ($L = 2$), 2 Rx-antennas are enough to support up to 20 users simultaneously, whereas for $L > 2$, more Rx-antennas are required as K increases so as to meet the 100ms D_p -constraint. Hence, provided with the same N_R for ICom/SIC-ZF, D_t of ZF grows as K increases when $L = 2$, but decreases with an increase of K when $L > 2$. In contrast, with ICom/SIC-ZF each user exclusively occupies W , and hence its D_t doesn't vary with K .

To make a further comparison, the difference of transmission delays, $\Delta D_t = D_t^{ZF} - D_t^{ICom/SIC-ZF}$ with $L = 64$, different K and V , is plotted in Fig. 13. Since a large L incurs more processing for the proposed strategy, the required N_R approaches K so as to meet the 100ms D_p -constraint. Thus, provided with the same N_R for both methods, ΔD_t decreases with the increase of L . Moreover, when $V \leq 0.1$ Mb, both D_t^{ZF} and $D_t^{ICom/SIC-ZF}$ are smaller than 2ms, i.e., ΔD_t is negligibly small relative to the D_p -constraint. For space limitation, we omit the results for other L s and $V < 0.1$ Mb. ΔD_t is shown to grow as V increases, i.e., for sessions with a larger volume of data, the proposed strategy becomes more advantageous in $D(t)$. Under the D_p -constraint, ICom/SIC-ZF requires more Rx-antennas as K increases, and thus N_R for ZF grows to achieve fairness. Then, D_t^{ZF} decreases with an increase of K due to the fact that a larger N_R provides

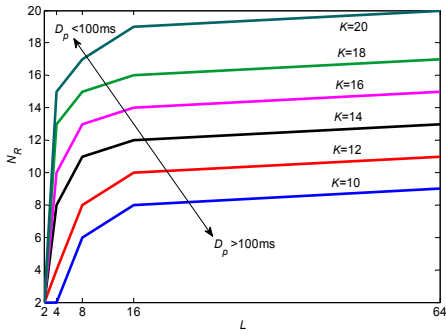


Fig. 11. Requirement of N_R under the 100ms D_p -constraint, different L and K .

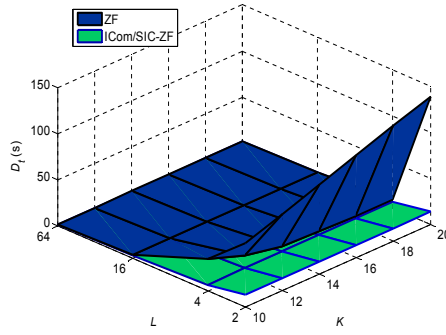


Fig. 12. Comparison of transmission delays under the 100ms D_p -constraint.

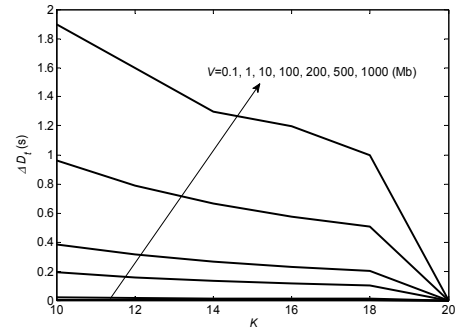


Fig. 13. D_t difference under $L = 64$, different K and V , and the 100ms D_p -constraint.

more DoFs for sharing. On the other hand, $D_t^{ICom/SIC-ZF}$ is independent of K , so ΔD_t shrinks as K increases. When $K = 20$ under $L = 64$, $N_R \geq 20$, the proposed scheme becomes the traditional ZF, and hence $\Delta D_t = 0$.

To summarize, under a certain D_p threshold, D_t of the proposed mechanism outperforms that of ZF, IA and IN for a large V and approximates them under small V values.

VI. CONCLUSION

In this paper, we proposed an ICom-based MAC-receiver structure employing ZF and SIC, namely ICom/SIC-ZF. By exploiting the constructive/destructive interactions among interfering signals, the dimension of interference can be reduced significantly. $K > N_R$ signals can then be decoded successively. With ICom/SIC-ZF, no Tx-side cooperation is required. All TxS send signals to the common Rx without any sacrifice for the others. By comparing it with other methods, the proposed reception mechanism is shown to achieve a remarkable improvement of system spectral efficiency, latency performance and flexible tradeoff between the requirement of Rx-antennas and computational complexity, thus facilitating the implementation of practical communication systems.

ACKNOWLEDGMENTS

This work was supported in part by NSFC (61173135, U14 05255, 61231008, 61102057); the 111 Project (B08038). It was also supported in part by the US National Science Foundation under Grant 1160775.

REFERENCES

- [1] T. Q. S. Quek, G. de la Roche, and M. Kountouris, "Small cell networks: deployment, PHY techniques, and resource management," Cambridge University Press, 2013.
- [2] T. Yoo and A. Goldsmith, "On the optimality of multi antenna broadcast scheduling using zero-forcing beamforming," *IEEE J. on Sel. Areas in Commun.*, vol. 24, no. 3, pp. 528-541, 2006.
- [3] M. Mollanoori, and M. Ghaderi, "Uplink scheduling in wireless networks with successive interference cancellation," *IEEE Trans. Mobile Computing*, vol. 13, no. 5, pp. 1132-1144, 2014.
- [4] V. R. Cadambe, and S. A. Jafar, "Interference alignment and spatial degrees of freedom for the k user interference channel," in *Proc. of the IEEE Int'l. Conf. on Commun. (ICC)*, pp. 971-975, 2008.
- [5] S. Mohajer, S. N. Diggavi, C. Fragouli, and D. N. C. Tse, "Transmission techniques for relay-interference networks," in *Proc. of the 46th Annual Allerton Conf. Commun., Control, and Computing*, pp. 467-474, 2008.
- [6] C. M. Yetis, T. Gou, S. A. Jafar, et al., "On feasibility of interference alignment in MIMO interference networks," *IEEE Trans. Sig. Process.*, vol. 58, no. 9, pp. 4771-4782, 2010.

- [7] H. Gao, J. Leithon, C. Yuen, et al., "New uplink opportunistic interference alignment: an active alignment approach," in *Proc. of the IEEE Wireless Commun. and Net. Conf. (WCNC)*, pp. 3099-3104, 2013.
- [8] C. Na, X. Hou, and A. Harada, "Two-cell coordinated transmission scheme based on interference alignment and MU-MIMO beamforming," in *Proc. of the IEEE Vehicular Technology Conf. (VTC)*, pp. 1-5, 2012.
- [9] B. Guler, and A. Yener, "Uplink interference management for coexisting MIMO femtocell and macrocell networks: an interference alignment approach," *IEEE Trans. Wireless Commun.*, vol. 13, no. 4, pp. 2246-2257, 2014.
- [10] I. Krikidis, "A SVD-based location coding for cognitive radio in MIMO uplink channels," *IEEE Commun. Lett.*, vol. 14, no. 10, pp. 912-914, 2010.
- [11] A. Zubow, M. Grauel, M. Kurth, and J. Redlich, "On uplink superposition coding and multi-user diversity for wireless mesh networks," in *Proc. IEEE Fifth Int'l Conf. on Mobile Ad-hoc and Sensor Networks*, pp. 403-411, 2009.
- [12] D. Jaramillo-Ramirez, M. Kountouris, and F. Hardouin, "Successive interference cancellation in downlink cooperative cellular networks," in *Proc. IEEE Int'l Conf. on Commun.*, pp. 5172-5177, 2014.
- [13] S. Gollakota, S. Perli, and D. Katabi, "Interference alignment and cancellation," in *Proc. of ACM SIGCOMM Conf. on Data Commun.*, pp. 159-170, 2009.
- [14] B. Shen, Z. Li, and Q. Liu, "Coexistent transmission and user scheduling for CR-MIMO system based on interference alignment and cancellation," in *Proc. of Annual Int'l. Symp. on Personal, Indoor, and Mobile Radio Commun. (PIMRC)*, pp. 403-407, 2013.
- [15] J. Zhang, Z. K. M. Ho, E. Jorswieck, et al., "SINR balancing for non-regenerative two-way relay networks with interference neutralization," in *Proc. of Int'l Conf. Acoustics, Speech and Sig. Process. (ICASSP)*, pp. 7604-7608, 2014.
- [16] D. Wu, C. Yang, T. Liu, et al., "Feasibility conditions for interference neutralization in relay-aided interference channel," *IEEE Trans. Sig. Process.*, vol. 62, no. 6, pp. 1408-1423, 2014.
- [17] J. Chen, A. Singh, P. Elia, et al., "Interference neutralization for separated multiuser uplink-downlink with distributed relays," in *Proc. of the Inf. Theory and Applications Workshop (ITA)*, pp. 1-9, 2011.
- [18] T. Gou, S. A. Jafar, C. Wang, et al., "Aligned interference neutralization and the degrees of freedom of the $2 \times 2 \times 2$ interference channel," *IEEE Trans. Inf. Theory*, vol. 58, no. 7, pp. 4381-4395, 2012.
- [19] O. Simeone, U. Spagnolini, Y. Bar-Ness, et al., "Distributed synchronization in wireless networks," *IEEE Signal Process. Mag.*, vol. 25, no. 5, pp. 81-97, 2008.
- [20] G. H. Golub and C. F. Van Loan, "Matrix Computations, 3rd ed.," Baltimore, MD: The John Hopkins Univ. Press, 1996.
- [21] I. Grigorik, "High performance browser networking," O'Reilly Media, 2013.
- [22] "TMS320TCI6612/14 High performance comes to small cell base stations," <http://www.ti.com/lit/ml/sprt610/sprt610.pdf>, 2011.
- [23] L. Gwennap, "Adapteva: more flops, less watts, epiphany offers floating-point accelerator for mobile processors," *The Linley Group Microprocessor Report*, pp. 1-5, 2011.
- [24] M. S. Gast, "802.11ac: a survival guide," O'Reilly Media, 2013.
- [25] C. Simon and G. Leus, "Round-robin scheduling for orthogonal beamforming with limited feedback," *IEEE Trans. Wireless Commun.*, vol. 10, no. 8, pp. 2486-2496, 2011.